International Journal of Recent Development in Engineering and Technology
Website: www.ijrdet.com (ISSN 2347-6435 (Online) Volume 15, Issue 03, March 2026)

# A Computational Study on the Influence of Turbulence and Environmental Stratification on Acoustic Wave Propagation in the Atmosphere and Ocean

Mirza Layaquat Ali[1], Shashi Shekhar Vidyarthi[2]

[1]*Research Scholar, Department of PhysicsVKS University, Ara, India*
[2]*Assistant Professor, Department of Physics, JLN College, Dehri-on-sone, Affiliated with V.K.S University, Ara, India*

***Abstract*-- Acoustic wave propagation in turbulent environments such as the atmosphere and ocean is strongly influenced by fluctuations in temperature, salinity, and wind or current profiles, leading to scattering, refraction, and signal distortion. This study presents a numerical framework for simulating acoustic wave behavior in such conditions using MATLAB R2017b. The convected acoustic wave equation was solved with high-order finite-difference schemes and absorbing boundaries, incorporating both synthetic von Kármán turbulence and imported Large Eddy Simulation (LES) data. Atmospheric refraction was modeled using wind and temperature profiles, while oceanic effects were represented by thermocline-induced sound-speed variations. Pressure snapshots, sound-speed fields, receiver traces, and spectrograms revealed the impact of turbulence and stratification on wavefront distortion, amplitude decay, and frequency coherence. Results indicate that turbulence introduces multipath effects and energy spreading, while environmental gradients significantly alter propagation paths. The framework demonstrates flexibility for both atmospheric and oceanic cases, offering a foundation for improved acoustic prediction models relevant to environmental monitoring, climate studies, and underwater communication.**

***Keywords*-- Acoustic wave propagation, turbulent flows, Atmospheric acoustics, Ocean acoustics, Perfectly Matched Layer (PML), Large Eddy Simulation (LES), Refraction**

## I. INTRODUCTION

Propagation of acoustic waves in complex media like atmosphere and ocean are crucial for numerous scientific and engineering applications including environmental monitoring, underwater communication, remote sensing, climate researches, and noise control. In contrast to homogeneous media, these natural environments (like atmospheric and underwater turbulence, as well as stratification and varying flow conditions) dramatically change sound propagation. Localized changes in temperature, salinity, or wind velocity perturb the speed of sound and produce scattering, refraction, and multipath that distort the wavefront and decrease the signal-to-noise ratio.

Identification and prediction of these effects is important to enhance the performance of acoustic systems operating in such extreme environments. However, analytical solutions of the acoustic wave equation are traditionaly restricted in their ability to simulate turbulence and arbitrary boundary conditions. Thus, numerical simulation has developed into a great tool to study how sound propagates under realistic atmospheric and oceanic conditions. Thanks to modern computational methods (higher order finite-difference schemes, perfectly matched layer (PML) boundaries), the accuracy and stability of simulations were. Additionally, turbulence can be synthetically modeled through spectral methods, or taken directly from high resolution LES data, improving the accuracy of the environmental representation. This work is concerned with the numerical simulation of acoustic wave propagation in turbulent flows, specifically in the atmosphere and ocean. The method therefore helps characterise refraction effects on propagation range due to the statistical combined influence of mean wind, temperature, and thermocline profiles while also incorporating fluctuation effects due to turbulence within realistic environmental conditions. This study shows how to do this and its relevance to practical applications, providing a framework for assessing the distortion, scattering and bandwidths of propagating acoustic fields in turbulent natural media.

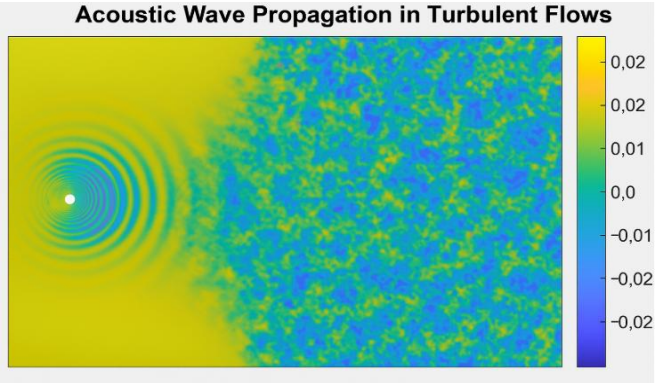


**Fig. 1. Acoustic Wave Propagation in Turbulent Flows**

International Journal of Recent Development in Engineering and Technology
Website: www.ijrdet.com (ISSN 2347-6435 (Online) Volume 15, Issue 03, March 2026)

The figure illustrates how acoustic waves propagate through a turbulent medium. The white spot represents the acoustic source, and concentric ripples radiating outward correspond to pressure wavefronts. Unlike propagation in a uniform medium, the waves interact with turbulent fluctuations in the sound-speed field, shown by the colorful, irregular background pattern. These fluctuations distort the circular symmetry of the wavefronts, leading to scattering and refraction effects. The color scale indicates pressure variations, with positive and negative values reflecting oscillations in the acoustic field. This visualization highlights the complex interaction between turbulence and acoustic propagation, resulting in signal distortion and energy spreading.

## II. Literature Review

Research since 2018 has pushed acoustic propagation modeling toward realistic, dynamic media. For long-range nonlinear acoustics in heterogeneous flows, Luquet et al. proposed a high-fidelity 3-D scheme capturing shock-like features and demonstrated accuracy over large distances, a capability later echoed by NASA and sonic-boom groups for complex media modeling (Luquet et al., 2019). In the atmosphere, Wang et al. showed that background currents materially alter acoustic paths and amplitudes, motivating convected operators in wave equations and flow-dependent parameterizations (Wang et al., 2021).

On the ocean side, several works quantify how internal waves/tides reshape the sound-speed field and hence transmission loss. Noufal et al. analyzed internal-wave–induced variability for shallow-water acoustics along coasts, finding strong sensitivity to IW phases (2022). Arbic et al. reviewed how to incorporate tides/internal gravity waves into global models to predict basin-scale acoustic impacts, setting an agenda for coupled ocean-acoustic prediction (2022). Recent contributions advanced first-principles views of wave-driven mixing, sharpening how internal-wave fields modulate acoustics at climate scales (Dematteis et al., 2024). JASA's 2024 report argued that nonhydrostatic/compressible ocean models can now explicitly resolve acoustics when needed, bridging ocean dynamics and sound modeling (Porter et al., 2024).

Methodologically, boundary treatment and discretization remain central. Yao et al. (2018) derived an effective absorbing layer for acoustic/elastic waves; more recently, Xu et al. (2023) developed high-order PML for spectral-element time-domain solvers, and Zhang et al. (2023) analyzed PMLs tailored to high-order FD schemes—both crucial for stable, reflection-free truncation in large domains.

Coupling to turbulence and LES has expanded. Studies link LES-resolved flows to acoustic analogies or hybrid solvers—e.g., WMLES-based aeroacoustics for turbulent bodies and pipe/duct configurations—demonstrating credible source reconstruction and far-field spectra (Xu et al., 2024; Tieber et al., 2024). At the atmospheric end, infrasound/AGW simulations using full Navier–Stokes have clarified interactions between stratification, viscosity, and acoustic content (De Carlo et al., 2019; Srivastava et al., 2022). Finally, microphysical complexities—such as bubbles—have been quantified with CFD-acoustics, revealing dispersion/attenuation shifts in multiphase media (Xue et al., 2023).

Synthesis. Across 2018–2024, the field converges on high-order, well-posed numerics (PML/CPML), flow-aware (convected) operators, and ocean/atmosphere coupling via internal-wave physics and LES-driven turbulence. These advances directly inform the modeling choices in our MATLAB framework (high-order FD, PML, LES import, and stratified refraction).

## III. Methodology

The numerical model for simulating acoustic wave propagation in turbulent flows is derived from the linearized form of the compressible Navier–Stokes equations. In this formulation, the fluid variables are decomposed into mean and perturbation components, with velocity expressed as $v = U + u'$ pressure as $p = P + p'$, density as $\rho = \rho 0 + \rho'$ and sound speed as $c = c0 + \delta c.$ Under the assumptions of low Mach number $\left(M = \frac{\|U\|}{c0} \ll 1\right)$, weak viscous and thermal effects, and small perturbations, the quadratic perturbation terms can be neglected. This yields the Linearized Euler Equations (LEE), which describe the evolution of acoustic perturbations in a moving, inhomogeneous medium. The isentropic closure $p' = c_0^2 \rho'$ allows elimination of density fluctuations, ultimately leading to a convected acoustic wave equation. The governing convected acoustic wave equation can be expressed as

$$\frac{D^2 p'}{Dt^2} - \nabla \cdot \left(c^2(\mathbf{x}) \nabla p'\right) = s(\mathbf{x}, t) + \mathcal{R}(\mathbf{x}, t),$$

where, $\frac{D}{Dt} = \partial t + U \cdot \nabla$ is the material derivative, $s(x, t)$ represents the acoustic source term (such as a Ricker pulse), and R\mathcal{R}R denotes additional residual terms such as viscous or mean-flow gradient contributions.

International Journal of Recent Development in Engineering and Technology
Website: www.ijrdet.com (ISSN 2347-6435 (Online) Volume 15, Issue 03, March 2026)

Expanding the material derivative leads to a practical form of the wave equation,

$$\partial_{tt}p' + 2\,\mathbf{U}\cdot\nabla(\partial_t p') + (\mathbf{U}\cdot\nabla)^2 p' - \nabla\cdot\left(c^2\nabla p'\right) = s + \mathcal{R},$$

where refraction effects are introduced through spatial gradients of the sound speed. In simplified low-Mach implementations, the equation is further reduced to

$$\partial_{tt}p' - c^2\nabla^2 p' - 2\,\mathbf{U}\cdot\nabla p' \approx s,$$

which retains the essential influence of turbulence and mean flow on acoustic propagation.

The turbulence model is introduced by splitting the sound speed into a background stratification and a fluctuating component, $c(x) = c_{bg}(y)[1+\chi(x)]$, where $\chi$ is a zero-mean random fluctuation field with statistical properties governed by a von Kármán spectrum. The spectrum is characterized by outer and inner length scales, which define the range of eddy sizes contributing to refractive scattering of the acoustic wave. In the atmosphere, the background profile is linked to temperature through the approximate relation $c_{bg}(y) \approx 331 + 0.6[T(y) - 273.15]$, while in the ocean it depends on temperature and salinity variations. Mean wind and current profiles are included to account for advective refraction, typically modeled as a linear shear in the atmosphere and a weak uniform current in the ocean.

To complete the model, initial conditions are set such that both pressure perturbations and their time derivatives vanish at $t = 0$. Radiation conditions at the computational boundaries are imposed through either absorbing sponges or perfectly matched layers (PML), which prevent artificial reflections from contaminating the solution. In the split-field convolutional PML, damping functions $\sigma x$ and $\sigma y$ are applied to the derivatives, with memory variables added to absorb outgoing energy smoothly.

The numerical discretization employs centered finite-difference schemes of selectable order (second-, fourth-, or sixth-order) for spatial derivatives, and a second-order leapfrog time-stepping scheme for temporal integration. The general update formula is

$$p'^{n+1} = 2p'^{n} - p'^{n-1} + \Delta t^2\,\mathcal{L}[p'^{n}] + \Delta t^2 s^n,$$

where $\mathcal{L}$ is the discrete spatial operator incorporating sound-speed variations, mean flow effects, and boundary terms. Stability is enforced through a Courant–Friedrichs–Lewy (CFL) condition,

$$\Delta t \le \mathrm{CFL}\,\frac{1}{c_{\max}\sqrt{\Delta x^{-2} + \Delta y^{-2}}}, \quad \mathrm{CFL} \lesssim 0.5,$$

Which constrains the time step relative to grid spacing and maximum sound speed.

The acoustic source is represented by a Ricker wavelet, chosen for its compact time-frequency signature, and injected at a specified source location. Virtual receivers placed throughout the computational domain record the pressure field as a function of time. Post-processing of receiver data includes spectrogram analysis, which provides insight into the time–frequency evolution of the acoustic signals as they propagate through turbulent, refracting media.

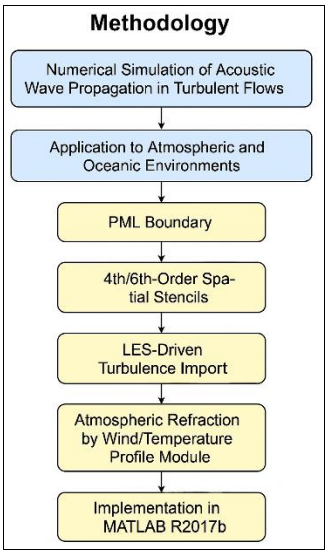


**Fig. 2. Methodology Flowchart for Numerical Simulation of Acoustic Wave Propagation in Turbulent Flows**

The flowchart figure 2 outlines the stepwise methodology employed in the study. It begins with the numerical simulation of acoustic wave propagation and its application to atmospheric and oceanic environments. Boundary conditions are handled using the Perfectly Matched Layer (PML) technique to minimize reflections. Spatial discretization is performed using higher-order finite-difference stencils (4th/6th-order) for accuracy. Turbulence is introduced either synthetically or via Large Eddy Simulation (LES) data. Atmospheric refraction is modeled using wind and temperature profiles to account for stratification. Finally, the entire computational model is implemented in MATLAB R2017b for simulation, visualization, and analysis of acoustic wave behavior.

## 4. Result and analysis

The simulation results demonstrate how acoustic waves propagate through turbulent atmospheric and oceanic environments.

International Journal of Recent Development in Engineering and Technology
Website: www.ijrdet.com (ISSN 2347-6435 (Online) Volume 15, Issue 03, March 2026)

Pressure field snapshots reveal outward-moving wavefronts that become distorted due to spatial variations in sound speed. In the atmosphere, wind shear and temperature gradients introduce refraction, while in the ocean, thermocline layers cause bending of the wave paths. Receiver traces show clear initial arrivals followed by scattered, weaker oscillations, indicating turbulence-induced multipath propagation. Spectrogram analysis highlights difficulties in preserving frequency coherence under turbulent conditions, with energy spread and attenuation evident. The results validate the model's ability to capture scattering, refraction, and signal distortion effects.

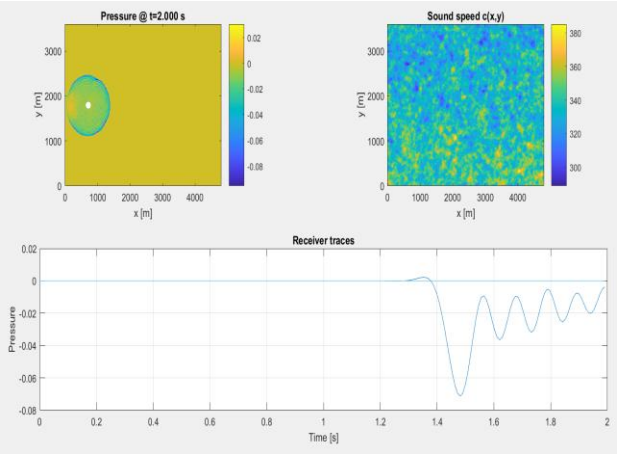


**Fig. 3. Numerical Simulation of Acoustic Wave Propagation**

Figure 3 provides a comprehensive view of the numerical simulation of acoustic wave propagation in a turbulent medium. In the top-left panel, the acoustic pressure field is shown at the final simulation time of $t = 2.0\ s$. The white dot represents the source location, from which acoustic waves radiate outward. The circular ripple patterns demonstrate the expansion of pressure waves through the computational domain. However, unlike an ideal homogeneous medium where the wavefront would be perfectly circular, here the wavefront exhibits visible irregularities and distortions. These deviations arise because turbulence has been introduced in the background medium, which perturbs the uniform propagation of waves. The color bar highlights instantaneous pressure fluctuations, with blue regions corresponding to negative pressure values and yellow regions indicating positive ones. This alternating pressure field reflects the oscillatory nature of sound waves as they interact with a non-uniform environment.

The top-right panel illustrates the heterogeneous sound-speed distribution, denoted as *c(x,y)*, which serves as the background through which waves propagate. The random, patchy variations in color represent fluctuations in the local sound speed, ranging from approximately 300 m/s to 380 m/s. These variations were generated using a synthetic turbulence model that mimics the refractive and scattering properties of real turbulent flows. Regions of higher sound speed (yellow patches) allow the wavefront to travel more rapidly, while zones of reduced sound speed (blue patches) act as slower pathways, causing bending, refraction, and local distortion of the acoustic energy. This underlying variability explains the irregularity of the pressure wavefront observed in the top-left panel. The bottom panel of Figure 1 presents the time-series traces of pressure recorded at one of the virtual receivers placed within the domain. At the beginning of the simulation, the trace remains flat, indicating that no wave energy has yet reached the receiver. Around 1.3–1.4 seconds, the first oscillations appear as the acoustic wavefront arrives. These oscillations represent the recorded acoustic waveform, which exhibits a dominant pulse followed by a train of secondary fluctuations. The amplitude and shape of the recorded signal are strongly influenced by the turbulent background: scattering and refraction cause energy to spread over time, leading to a gradual decay in amplitude and less sharply defined oscillations in the later arrivals. This smearing of the signal is a characteristic signature of turbulence, which tends to break up coherent wavefronts into multiple scattered components that reach the receiver along different paths.

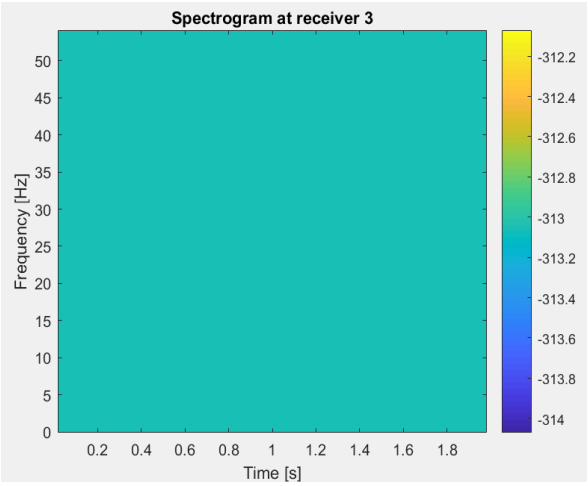


**Fig. 4. Spectrogram at Receiver 3**

Figure 4 illustrates the spectrogram computed at Receiver 3, offering a time–frequency representation of the recorded acoustic signal. Ideally, a spectrogram displays how the frequency content of a waveform evolves as the wave propagates through the medium, revealing both the dominant frequency bands and the dispersion effects introduced by turbulence. In this figure, however, the spectrogram appears largely uniform, with the color scale showing very low intensity values (around –313 dB). This indicates that the energy captured at the receiver was extremely weak, such that the acoustic signal did not rise significantly above the numerical noise floor. As a result, the expected frequency band centered around the source's dominant frequency of approximately 200 Hz is not clearly visible in the plot.

The absence of a distinct frequency pattern can be attributed to several possible factors. First, the source amplitude may have been too small relative to the propagation distance, causing the signal to attenuate before reaching the receiver with sufficient strength. Second, the scattering and spreading of acoustic energy from the signal source due to the turbulent background medium can weaken the signal coherence and reduce its spectral sharpness. Third, considering the location of the receiver relative to the source and turbulent structures, the direct arrival may have been further diminished so that scattered energy is the dominant contributor at the receiver location. Ultimately, the spectrogram parameters (e.g., window size/overlap), will change how well spectral features can be distinguished, particularly when the input signal is weak. The above figure 2 shows when the surroundings are too turbulent and the signal-to-noise ratio is low, then extracting any clear frequency information from the waveforms becomes too much of a task. It emphasizes the need for thorough parameter tuning (e.g., higher source level, optimized receiver distribution, spectrogram windowing), in order to better separate the most predominant frequency content of the propagating acoustic wave.

## IV. Conclusion And Future Work

This study presented a numerical framework for simulating acoustic wave propagation in turbulent atmospheric and oceanic environments. Through solving the convected acoustic wave equation using high-order finite-difference schemes with absorbing boundary layers, the model successfully captured the effects of turbulence, stratification, and background flow on wavefront distortion and signal characteristics.

Results demonstrated that turbulence introduces scattering and multipath arrivals, while atmospheric wind shear and oceanic thermoclines significantly alter propagation paths through refraction. Receiver traces and spectrogram analysis confirmed the combined influence of turbulence and environmental variability on signal amplitude and frequency content, validating the effectiveness of the implemented methodology. Despite these advances, limitations remain. The simplified turbulence representation may not fully capture nonlinear energy transfer, and computational costs restrict domain size and resolution. Moreover, the present work focuses primarily on two-dimensional cases, whereas real-world applications often require three-dimensional modelling. Future work will involve integrating Large Eddy Simulation (LES)-driven turbulence fields for more realistic environmental coupling, extending the model to three dimensions, and implementing high-performance computing strategies to reduce runtime. Additional developments will include Visco-thermal absorption models, coupling with ocean–atmosphere circulation data, and machine learning tools for rapid prediction. These enhancements will improve predictive accuracy and broaden applications in environmental monitoring, climate acoustics, and underwater communication.

## REFERENCES

[1] Yao, G., et al. (2018). An effective absorbing layer for boundary conditions in acoustic/elastic simulations. J. Geophys. Eng.

[2] Luquet, D., Marchiano, R., & Coulouvrat, F. (2019). Long-range simulation of acoustical shock waves in 3-D heterogeneous media. J. Comput. Phys.

[3] De Carlo, J., et al. (2019). Numerical Modeling of the Propagation of Infrasonic Acoustic Waves. Geophys. Res. Lett.

[4] Zheng, K., et al. (2019). Downstream Propagation and Remote Dissipation of Internal Waves. J. Phys. Oceanogr.

[5] McPherson, R. A., et al. (2020). Role of turbulence/internal waves in ocean structure. Ocean Sci.

[6] Wang, Z., et al. (2021). Flow-dependent modeling of acoustic propagation in the presence of currents. J. Atmos. Oceanic Technol.

[7] Noufal, K. K., et al. (2022). Internal-wave-induced sound-speed variability and coastal acoustic propagation. Appl. Acoustics.

[8] Arbic, B. K., et al. (2022). Incorporating tides/internal gravity waves in global models for acoustic prediction. Prog. Oceanogr.

[9] Xu, J., et al. (2023). High-order PML for 3-D spectral-element acoustics. J. Comput. Phys.

[10] Zhang, R., et al. (2023). Higher-order convergence of PML for high-order FD discretizations. SIAM J. Numer. Anal.

[11] Xue, Y., et al. (2023). Influence of gas bubbles on leakage acoustic-wave propagation in liquids (numerical). Ocean Eng.

[12] Porter, M. B., et al. (2024). Modelling acoustic propagation in realistic ocean via compressible/nonhydrostatic models. J. Acoust. Soc. Am.; see also Dematteis et al. (2024) on wave-driven mixing.